A dynamic absorber with a soft magnetorheological elastomer for powertrain vibration suppression

N Hoang[1, 2]**, N Zhang**[1] **and H Du**[1]

[1]School of Electrical, Mechanical and Mechatronics Systems, Faculty of Engineering University of Technology, Sydney, PO Box 123, Broadway, NSW 2007, Australia

[2]Institute of Mechanics, 264 Doican, Hanoi, Vietnam

E-mail: Nga.Hoang@eng.uts.edu.au

Abstract. This paper presents a conceptual adaptive tunable vibration absorber (ATVA) with soft magnetorheological elastomers (MREs) for vibration reduction of vehicle powertrain systems. The MRE material used in this application has a rubbery silicone polymer matrix and ferrous fillers in fraction of 27.6% by volume. For such a soft MRE the elastic modulus significantly increases due to the MR effect. Thus, the ATVA can work effectively in a wide frequency range (the increase in frequency more than 10 times) instead of a narrow bandwidth as a conventional dynamic absorber does. Numerical simulations of a powertrain fitted with the ATVA are used to validate its effectiveness. The obtained results show that the powertrain vibration can be significantly suppressed. This novel ATVA will be applicable to the vibration reduction of powertrains.

Keywords: Adaptive tunable dynamic absorber, vibration reduction, powertrain vibration, soft magnetorheological elastomer.

1 Introduction

Magnetorheological elastomers (MREs) are a smart material in the MR family including MR fluids, foams and elastomers. Typically, MREs are composed of a host gel material and micro-size iron additives. One vital MRE feature of MREs called MR effect is that their mechanical properties such as elastic moduli (including Young's modulus E as well as shear modulus G) can be properly controlled by a magnetic field [1, 2]. Thus, MREs have been a promising material for constructing adaptive tuned vibration absorbers (ATVAs), which are effective devices to absorb the undesirable vibration of mechanical systems whose natural frequencies coincide with or are close to the forcing frequency. Generally, the increment in elastic modulus in regular MREs under MR effect is about 50-60 % [1, 2, 3]. However, the increment may seem to be insufficient for the purpose of constructing ATVAs for systems having a wide range of natural frequency such as vehicle powertrain systems.

In recent years, there have been an increasing number of studies about how to broaden MRE's stiffness range. Farshad and Benine [4] developed a magnetoactive elastomer and they pointed out that the maximum increase in tensile modulus and compression modulus is 200% for the former and more than 300% for the latter. Zhang et al [5] proposed a theoretical model for a new MRE, which is enhanced by magnetizable soft material in nano size so that its shear modulus could be significantly increased. Stepanov et al [6] introduced the tangential Young's modulus for describing the non-linear behaviour of a new soft MRE. Their experimental results showed that for the MRE sample, with the magnetic filler content by volume 37%, the maximum increase in the modulus, when strain is small (less than 4%), is up to 100 times. In line with the result, Abramchuk et al [7] measured the shear modulus for a soft MRE in small strain regime. This MRE material is based on a silicone polymer matrix and the ferrous filler content by volume 27.6%. It seemed the first time the relationship between elastic modulus and magnetic field with the increase in shear modulus is about 10000% (100 times) is presented. The MRE sample will be used in this study to develop the ATVA.

A great number of studies have used MREs for constructing ATVAs. Deng et al [8] developed an ATVA for a beam with two ends supported. This ATVA could work effectively in a frequency range from 55 to 82 Hz with relative frequency change of 49%. Albanese and Cunefare [9] presented a state-switched absorber (SSA) using a MRE material and found that with iron particles by volume 35% the MRE material has the largest MR effect and the natural frequency of the SSA could be tuned from 45Hz to 183 Hz (360% increase in frequency shift). Lerner and Cunefare [10] tested the SSA operated in different working modes and the result showed that the increase in SSA's natural frequency range are 183% (26-74Hz), 473% (78-449Hz) and 510% (57-347Hz) in shear, longitudinal and squeeze mode respectively. However, a shortcoming is that so far the MRE has been used for developing ATVAs for single degree-of-freedom (SDOF) applications only. Actually, most real world structures and mechanisms have multi degrees of freedom (MDOF). This shortcoming limits the application of the unique MRE material to many engineering problems.

Ram and Elhay [11] showed the mathematic background of a MDOF dynamic absorber for MDOF systems. They also pointed out that the SDOF dynamic absorbers, which have been being used so far, are a particular instant of MDOF dynamic absorber. Hadi et al [12] used the genetic algorithm to optimize a dynamic absorber design for a MDOF system structure. Ozer and Royston [13] extended Den Hartog's method to find optimal parameters of dynamic absorber added to an undamped MDOF system. Ozer and Royston [14] applied Sherman-Morrison matrix inversion formula for optimisation parameters of a dynamic absorber attached to a damped MDOF system. Kitis et al [15] found optimal design of a damped absorber, which is added to a damped MDOF system. This finding bases on the numerical method and is demonstrated for a 22 DOF system in the case study. In contrast to studies in the paragraph above, there may have not been any work using the MRE for constructing ATVAs for MDOF applications.

A power transmission system (powertrain) is a crucial component in automobiles. It consists of an engine, a torque converter (TC) or a clutch for automatic or manual transmission, a transmission gear box and a drive line component including the differential, wheel tyres and vehicle body. In a vehicle powertrain there are a number of gear ratios, which are used to set the optimal engine speed according to vehicle speed. Due to gear shift of transmission, the stiffness coefficients depend on the output speed ratio of gear set. Thus, for each speed, the powertrain has a different set of natural frequency. Hwang et al [16] investigated a Ford rear-wheel automatic powertrain and these results indicate that the fundamental frequency versus axle stiffness is about 5.5Hz to 7.0 Hz for the third gear and 6.75 Hz to 8.0 Hz for the fourth gear. Zhang et al [17] and Crowther [18] studied transient and free vibration of an automatic powertrain BTR four-speed 93 LE. Their results pointed out the first powertrain fundamental frequency for the second gear is 7.0 Hz and for the third gear is 8.8 Hz. The second powertrain fundamental ones are 28.6Hz and 28.0Hz for the second and third gear respectively. Couderc et al [19] simulated and tested a manual powertrain and showed that the gear rattle vibration mode with frequency 68.3 Hz is potential vibration source. Obviously, there are many natural frequencies in a wide range of frequency in the system. In addition, the torque fluctuation is periodic due to the internal combustion engine dynamic characteristics so that the powertrain is subjected to multi-frequency excitations. Because the engine speed range is large the resonance phenomena may not be avoided. Especially, when the engine speed accelerates from 600-900 rpm (idle speed) to 5000-6000 rpm (top working speed) it will pass through several natural frequencies. Consequently, the vibration of the system could increase significantly if the acceleration time is not rapid enough and this vibration reduces the comfort performance of vehicle.

The objective of this study is to use the soft MRE material presented by Abramchuk et al [7] to develop a novel torsional ATVA for a simplified MDOF power transmission system. Based on the new MRE material, this device can be actively tuned according to the engine speed and the powertrain resonant frequency can be shifted away so that the powertrain vibration is significantly reduced. This novel ATVA will be an innovation in vibration reduction for powertrain systems. Numerical simulations of powertrain fitted with the proposed ATVA are conducted to validate its effectiveness. This paper consists of three main sections. The first section presents an introduction of the new MRE material and its characteristics. The second section proposes a conceptual design of the torsional ATVA. Finally, the third section presents numerical simulations to validate the ATVA effectiveness for powertrain vibration suppression.

2 A soft MRE and its characteristics

Abramchuk et al [7] presented a new soft MRE. The composition of the MRE is a highly elastic polymer and magnetic particles, which are filled to the polymer matrix. The magnetic fillers are ferrous powders whose sizes range from 2-3 μm .

The polymer matrix of the host material is a liquid silicone rubber, which is produced by GNIIKhTEOS (Institute of Chemistry and Technology of Organoelement Compounds, Russia)

The polymer matrix consists of two components. The first component is silicone oligomer with vinyl groups and the second one is silicone oligomer with hydride groups. The polymer matrix of the MRE is created by following chemical reaction with the presence of platinum as a catalyst.

$$\sim \mathrm{Si\text{-}CH{=}CH_2} + \mathrm{H\text{-}Si} \sim \xrightarrow{\text{Pt catalyst}} \sim \mathrm{Si\text{-}CH_2{-}CH_2\text{-}H\text{-}Si} \sim$$

The fabrication process of the MRE consists of three main steps. Firstly, the mixture of the silicone rubber and magnetic particles are pestled by a mechanical mortar. Secondly, the ferrous powder homogeneously dispersed in to the polymer matrix and the air bubbles are removed from the volume of sample. Finally, the mixture material was injected into moulds and is polymerised for two hours at temperature 100 to 150^0C for two hours.

It is assumed that the material is operated in the small strain regime and the relationship between Young's modulus and shear modulus in this regime is linear so that the tensile test is conducted and the shear modulus G can be calculated from following equation, [7]:

$$\sigma = G(\lambda - \frac{1}{\lambda^2}) \tag{1}$$

Where σ is the nominal stress; λ is the relative compression length $\lambda = l / l_0$; l is length of the deformed sample and l_0 is the initial length of undeformed length.

For a soft MRE sample that ferrous powders with volume concentration is 27.6%, σ and λ were measured under various magnetic fields and the shear modulus was calculated by equation (1). Figure 1 shows the relative changes in shear modulus (G/G_0), which depends on the magnetic field strength. It was obtained by mapping point-to-point and interpolated by Matlab software. In which G_0=3.5kPa is the initial shear modulus without magnetic field. It is noted that the relationship between G-H is displayed in the formation of logarithm (base 10), Abramchuk et al [7].

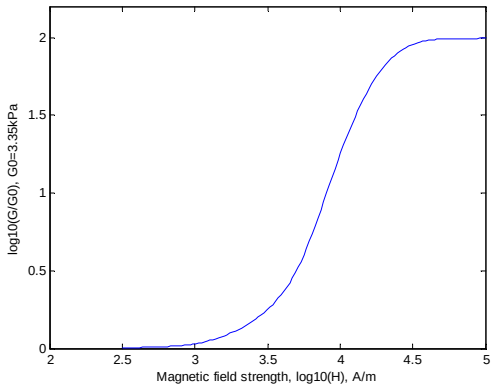

Figure 1. Relative shear modulus of soft MRE depending on magnetic field.

It is assumed that the field intensity strength H(the maximum value is 100kA/m) is produced by a magnetic field of coil with current I. Obviously, H depends on a number of factors such as turns of

wire, the type of material in the coil and the ratio of the coil length to the coil width. For convenience H is expressed in the form

$$H = \alpha I \tag{2}$$

Where α is the propositional coefficient. For instant, the magnetic field is assumed similar as one presented by Park et al, [20], α =12500/m was chosen, the relationship between the shear modulus G and input current I is shown in figure 2.

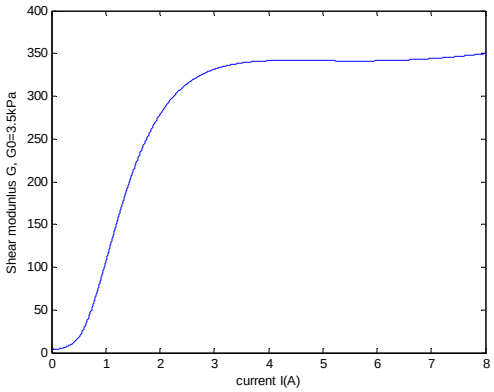

Figure 2. Shear modulus of soft MRE depending on input current I.

It is noted that that the increase in shear modulus is significant (more than 100 times).

3 A novel ATVA for powertrain vibration control

3.1 A simplified powertrain model and its vibration characteristics

A simplified torsional vibration model, which consists of inertias, stiffnesses and dampings as shown in figure 3, is used to validate the ATVA effectiveness. In which, the vehicle engine is modelled by the first inertia. The second and third inertias represent the torque converter (TC) and the gear box of transmission. The drive line components are modelled by the fourth inertia. This model is condensed from a powertrain test rig, which was reported by Zhang et al [17] and Crowther [18].

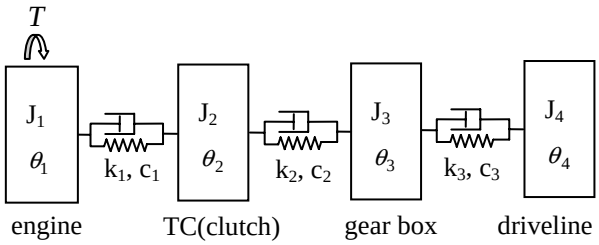

Figure 3. A simplified vehicle powertrain model.

By using Lagrange's equation it is straightforward to obtain equation of motion of the system as:

$$\mathbf{J}\ddot{\boldsymbol{\theta}} + \mathbf{C}\dot{\boldsymbol{\theta}} + \mathbf{K}\boldsymbol{\theta} = \mathbf{T} \tag{3}$$

Where $\boldsymbol{\theta} = \begin{bmatrix}\theta_1 & \theta_2 & \theta_3 & \theta_4\end{bmatrix}^T$, $\mathbf{T} = \begin{bmatrix}T & 0 & 0 & 0\end{bmatrix}^T$ are vectors of generalized coordinates and external torque; the inertial matrix **J** is diagonal, **J**=diag(J_1, J_2, J_3, J_4); stiffness and damping matrices, **K** and **C**, have following forms:

$$\mathbf{K}=\begin{bmatrix} k_1 & -k_1 & 0 & 0 \\ -k_1 & k_1+k_2 & -k_2 & 0 \\ 0 & -k_2 & k_2+k_3 & -k_3 \\ 0 & 0 & -k_3 & k_3 \end{bmatrix};\mathbf{C}=\begin{bmatrix} c_1 & -c_1 & 0 & 0 \\ -c_1 & c_1+c_2 & -c_2 & 0 \\ 0 & -c_2 & c_2+c_3 & -c_3 \\ 0 & 0 & -c_3 & c_3 \end{bmatrix} \quad (4)$$

When an ATVA or ATVAs are attached, the equation of motion of powertrain including ATVA keeps the same form as equation (3) but $\boldsymbol{\theta}$, **T**, **J, K** and **C** will be changed.

In this case study, the free and steady vibration of the system before and after adding the ATVA are investigated for the first, second, third and fourth gears associated with different speed ratios. These gears are characterized by varying the stiffness coefficient k_2. When the powertrain is in a resonant range, the ATVA is considered to work effectively if the powertrain natural frequencies could be shifted away from the resonant peaks so that powertrain steady responses is reduced significantly.

Let J_1=0.82, J_2=0.22, J_3=0.4, J_4=8kgm^2; c_1=1.0, c_2=2.0, c_3=5.0Nms/rad; k_1=15000, k_3=3350Nm/rad. Where k_2=13000, 15000, 16000 and 18000 Nm/rad for the first, second, third and fourth gear of gear box are used, respectively. Table 1 shows the powertrain natural frequencies and damping ratios ζ for the first, second, third and fourth gear of gear box.

Table 1. Natural frequencies of a simplified powertrain model for different gear shifts.

	first gear		second gear		third gear		fourth gear	
index	f (Hz)	ζ (%)	f (Hz)	ζ (%)	f (Hz)	ζ (%)	f (Hz)	ζ (%)
f_1	0[a]		0[a]		0[a]		0[a]	
f_2	7.5299[b]	2.89	7.5937	2.96	7.6199	2.99	7.6640	3.04
f_3	28.0366	3.27	28.7146[b]	3.05	29.0034	2.97	29.5017	2.82
f_4	62.3363	2.39	64.8331	2.35	66.0662	2.32	68.4972[b]	2.27

[a] the first natural frequency is zero due to the rigid body rotation of whole system (without vibration)
[b] powertrain natural frequencies are used to validate the ATVA effectiveness.

Although the powertrain natural frequencies vary for each gear shift, their vibration mode shapes have similar forms. For instant, figure 4 shows the powertrain vibration mode shapes of the first gear of gear box. It can be seen that the second mode is sensitive to either the first, second or third inertia. In other words, the second frequency powertrain can be shifted away if an ATVA is added to these inertias. Meanwhile, the third and fourth modes seem to be only sensitive to the third and second inertia, respectively. This will be discussed more details in section 4.2.

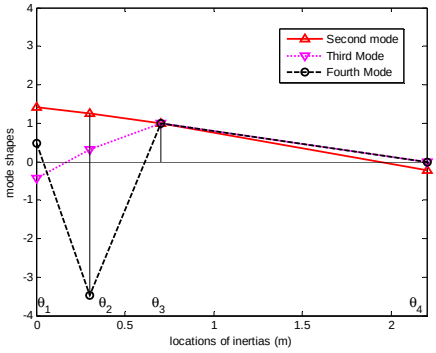

Figure 4. The second, third and fourth mode shapes of the first gear of gear box.

3.2 Structure of the proposed ATVA

The ATVA schematic diagram is shown in figure 5, in which the inner cylinder with lugs is fixed on the rotating shaft. The MRE material operates as a torsional spring and it is put into the gap between the inner and outer cylinder. Like the inner cylinder, there are lugs on the outer cylinder. These lugs cause tangent elastic forces as well as elastic torque between these cylinders. Therefore, the outer cylinder can vibrate to the inner cylinder. There are three electromagnetic coils, which are supplied by a DC current to make a magnetic field through the MRE layer.

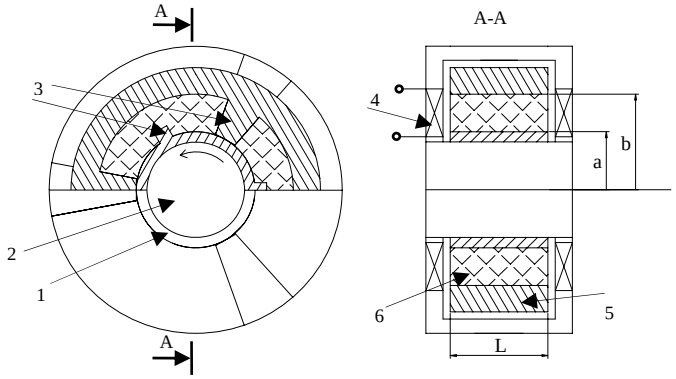

Figure 5. A schematic diagram of the ATVA.1: inner cylinder; 2: rotating shaft; 3: lug; 4: electromagnetic coils; 5: outer cylinder; 6: MRE material.

If the MRE plays a role as a torsional spring and is modeled as a rubber cylinder with inner, outer radius and length as a, b and L, respectively as shown in figure 5, the torsional stiffness coefficient of MRE can be calculated as, [21]:

$$k_A = \frac{4\pi L a^2 b^2 G}{b^2 - a^2} \tag{5}$$

Let J_A be ATVA's effective inertia moment and it can be calculated by:

$$J_A = \int r^2 dm = \sum mr^2 \tag{6}$$

Where r and dm are the moment arm and element of mass.

It is noted that the mass of MRE material can be neglected due to it is very small versus that of outer ring and wire coils. The ATVA's effective inertia moment could be calculated:

$$J_A \approx J_{outter\ ring} + 3J_{Wire} = mb^2 + 3m_{Wire}d^2 = m(b^2 + \frac{3m_{Wire}}{m}d^2) = mR_0^2 \tag{7}$$

Where m, m_{Wire} are masses of the outer ring and one wire coil, respectively; d is the distance from the mass centre of coil to the rotating shaft centre; R_0 is the radius of gyration and it can be calculated by:

$$R_0^2 = b^2 + \frac{3m_{Wire}}{m}d^2 \tag{8}$$

Because parameters m, m_{Wire}, b, d, R_0 is relatively independent, each of them can be obtained easily from the others. For example with m=1kg, b=0.1m, m_{Wire}/m=0.3086, d=0.18m are given, R_0=0.2m, J_A=0.04kgm^2 and μ_A=0.1 will be calculated. For more convenience, the inertia ratio $\mu_A = J_A / J_3$ is varied to investigate the ATVA effectiveness in the design stage.

ATVA natural frequency and damped frequency are calculated by:

$$f_A = \frac{1}{2\pi}\sqrt{\frac{k_A}{J_A}} \tag{9}$$

$$f_d = f_A\sqrt{1-\varsigma_A^2} \tag{10}$$

ς_A is the damping ratio of the MRE material.

In general, the damping property of MREs depends on several factors, [1, 3, 23]. Chen et al, [23], tested MRE samples under various magnetic fields, polymer matrices, and dynamic strain regimes and reported that when magnetic field increases, the damping ratio slightly increases until reaching a maximum value at first and then it decreases slightly. In addition, the damping ratio is always less than 0.35. This study seems the most comprehensive study about the MRE damping property so far. However, there has not been any MRE sample that is similar to the soft MRE used for our work. Zhou, [3] tested a MRE with 27% ferrous powders by volume embedded in a silicone rubber matrix and showed that the damping ratio is a slightly decreasing line (about 10%) when the magnetic field increases. The zero-field damping ratio ς_{A0}=0.24 was measured. Due to the MRE damping property used in this work has not given yet, the damping model reported by Zhou, [3], will be used. That means the damping ratio can be expressed as $\varsigma_A = \varsigma_A(I) = \varsigma_{A0} - \eta I$, η is the coefficient. If a decline of the damping ratio 10%, i.e., $\frac{\varsigma_{A\min}}{\varsigma_{A\max}} = 9/10$ was set, $\eta = \frac{\varsigma_{A0}}{10I_{\max}}$ will be calculated and the damping ratio can be expressed as:

$$\varsigma_A = \varsigma_{A0} - \frac{\varsigma_{A0}}{10I_{\max}}I = \varsigma_{A0}(1-\frac{I}{10I_{\max}}) \tag{11}$$

In this study, four zero-field damping ratio ς_{A0}=0.05, 0.10, 0.25 and 0.35 were used to investigate the ATVA effectiveness. The characteristics of the four kinds of damping ratio are shown in figure 6.

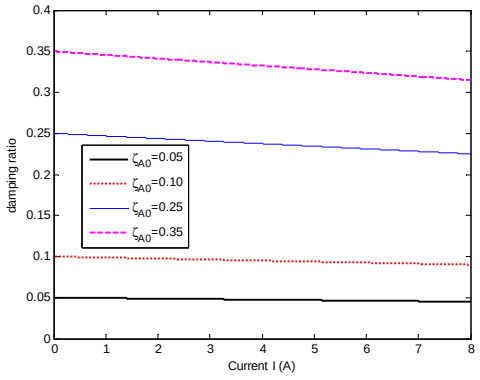

Figure 6. ATVA damping ratios for ς_{A0}=0.05, 0.10, 0.25 and 0.35.

If a damping ratio ς_A is selected, the ATVA damping coefficient can be calculated:

$$c_A = \varsigma_A C_c \tag{12}$$

$C_c = 4\pi f_A J_A$ is the critical damping coefficient.

When the ATVA is added to the powertrain, J_A is fixed and current I is tuned for controlling ATVA damped frequency f_d (both k_A, c_A are tuned by I at the same time). The conversion among ATVA main parameters such as k_A, G, f_A, f_d, I, ς_A, c_A is through equations (5), (9), (10), (11) and (12).

It is noted that the powertrain frequency range is from f_{min}=7.5299Hz to f_{max}=68.4972Hz as Table 1. In this study ATVA main parameters are shown in Table 2.

Table 2. ATVA's parameters.

Inertial moment and geometry	MRE material	Magnetic field
μ_A =J_A/J_3=1/4, 1/5, 1/10, 1/20	G_0=3.50kPa	α =12500/m
a=0.085m	G_{max}=350kPa	I_{max}=8A
b=0.100m	ς_{A0} =0.05, 0.10, 0.25, 0.35	H_{max}=100kA/m
L=0.075m		

Figure 7 shows the ATVA's frequencies which depend on the input current I for the four damping ratio characteristics and the inertia ratio μ_A =1/10 was set.

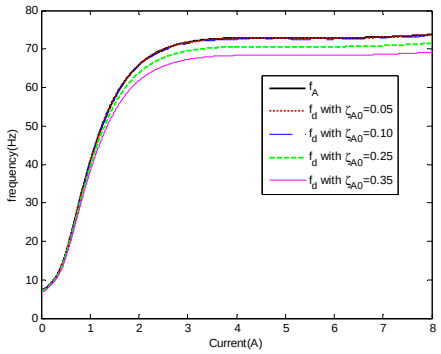

Figure 7. ATVA's frequency range for four damping ratio characteristics for μ_A =1/10.

It is noted that the ranges of f_A and f_d for ς_{A0} =0.05, 0.10 are [7.3756 73.7475], [7.3664 73.6728] and [7.3387 73.4482] (Hz), respectively. For such zero-field damping ratios the difference between f_A and f_d is very slight while the frequency ranges for ς_{A0} =0.25 and 0.35 are [7.1415 71.8565], [6.9094 69.9931] (Hz) and the difference is significant. Obviously, with the parameters as designed, the ATVA frequency ranges covered that of powertrain (with [f_{min} f_{max}]=[7.5299 68.4972] (Hz)).

4 Numerical simulations

4.1 Parameter influence on ATVA effectiveness, a case study for the first gear of gear box

According to Wang et al [22], engine torque could be given as

$$T = T_m + T_0 \sin(\Omega t) \tag{13}$$

Where T_m is the constant mean torque. T_0 and Ω are the amplitude and frequency of fluctuation torque. In this study, only fluctuation torque is considered and T_m is neglected. The forcing frequency Ω depends on number of cylinders and engine speed. It is assumed that Ω is a half of engine frequency. If the engine is at idle speed (about 900rpm) it gives $\Omega = 2\pi \times 7.5$ (rad/s). When the first

gear of gearbox is operated, the resonance may occur to the second frequency f_2=7.5299Hz of the first gear as noted in Table 1. Thus, an ATVA is attached to powertrain as in figure 8. With the ATVA, the system has five degrees of freedom and the equation of motion has the same form as equation (3). Where $\boldsymbol{\theta} = [\theta_1 \ \ \theta_2 \ \ \theta_3 \ \ \theta_4 \ \ \theta_A]^T$, **J**=diag($J_1$, J_2, J_3, J_4, J_A) and the stiffness matrix has form as:

$$\mathbf{K} = \begin{bmatrix} k_1 & -k_1 & 0 & 0 & 0 \\ -k_1 & k_1 + k_2 & -k_2 & 0 & 0 \\ 0 & -k_2 & k_2 + k_3 + k_A & -k_3 & -k_A \\ 0 & 0 & -k_3 & k_3 & 0 \\ 0 & 0 & -k_A & 0 & k_A \end{bmatrix} \tag{14}$$

The damping matrix **C** has the same form as the stiffness matrix **K.**

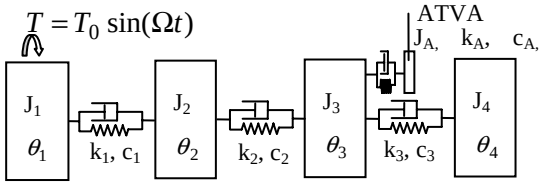

Figure 8. A powertrain model with an ATVA.

For the powertrain frequency f_2=7.5299Hz, let ς_{A0}=0.1, μ_A=1/4 so that the current is converted as I=0.072A. In practise, I=0.05A or I= 0.1A is chosen, and f_d=7.433Hz or f_d=7.7139Hz is obtained. For instant, I=0.05A (f_d=7.433Hz) is tuned and the vector of powertrain natural frequencies **f** = [0.0 6.8639 8.1554 28.2069 62.3467]^T are re-calculated. Comparing to those in Table 1, the powertrain frequencies have been shifted away from the resonant peak f=7.5299 Hz by introducing two new frequencies 6.8639 and 8.1554(Hz). Let T_0=3Nm, the powertrain steady responses before and after adding the ATVA are shown in figure 9.

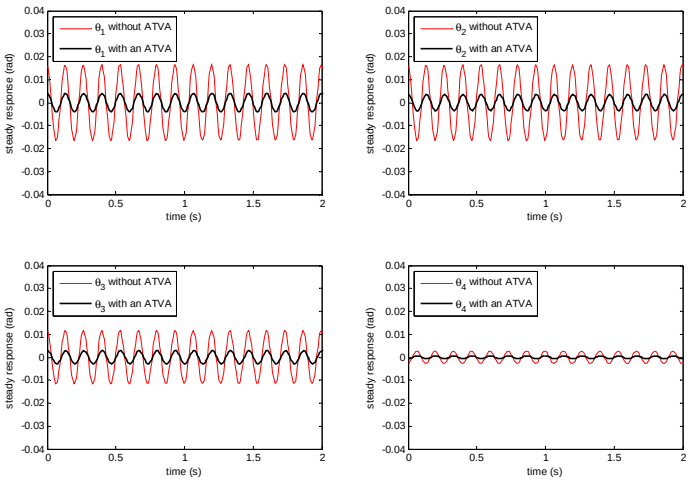

Figure 9. Steady state responses at current I =0.05A, ς_{A0}=0.1, μ_A=1/4.

Obviously, the vibration of the four inertias, $\theta_1, \theta_2, \theta_3$ and θ_4 are reduced significantly after adding ATVA. This confirms that the ATVA works as designed.

To illustrate the effectiveness of ATVA over a forcing frequency range, the powertrain vibration frequency response was shown in figure 10. The forcing frequency ratio Ω/ω_d is from 0.6 to 1.4. That means the forcing frequency range is [0.6 1.4]f_d= [4.4598 10.4062] (Hz).

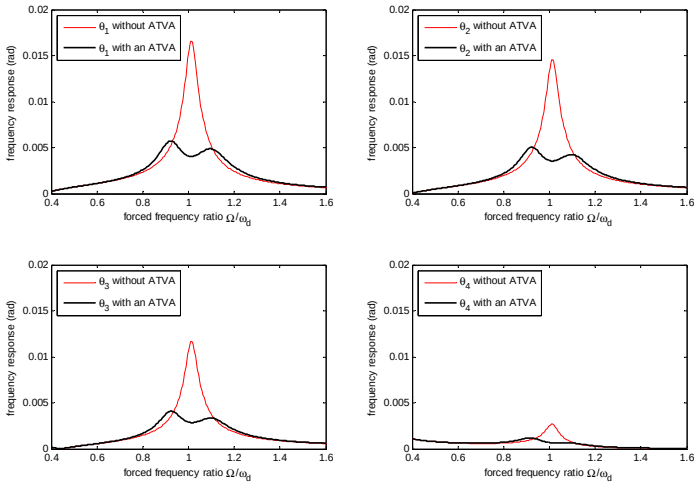

Figure 10. Frequency responses when ς_{A0}=0.1, μ_A=1/4.

It is oblivious that vibration frequency responses are reduced significantly at and around the resonant frequency f_d (at the forcing frequency ratio, Ω/ω_d , is close to 1) when ATVA is added to powertrain. To show how the inertial moment J_A affects to the effectives of ATVA, the inertia ratios μ_A=1/4, 1/5, 1/10, 1/20 was varied. For the zero-field damping ratio ς_{A0}=0.1 was chosen, the responses of second inertia are shown in figure 11.

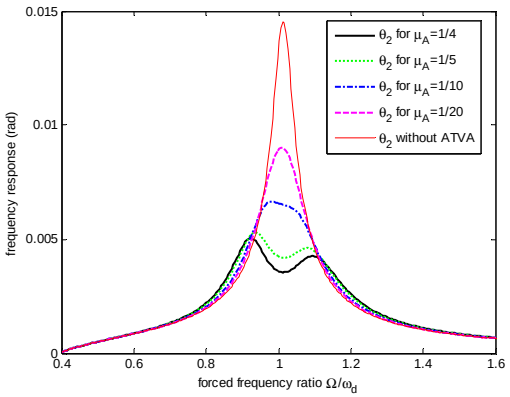

Figure 11. Frequency responses of the second inertia θ_2 for several values of inertia ratios μ_A.

It can be seen that the larger inertia ratio, the better vibration reduction effect the ATVA can be. For large inertia ratios large such as μ_A=1/4, μ_A=1/5 the resonant peak is shifted far away by introducing two new invariant peaks. Thus, the responses are suppressed significantly while for low inertia ratios μ_A=1/10 or 1/20 it is not so that the vibration at the resonant frequency are reduced not much as can be seen in figure 11.

To show how the input current, I, affects the powertrain responses, the responses with several input current values are calculated and compared. It is noted that if input current I varies, both stiffness and damping coefficients will be changed. Figure 12 shows responses of second inertia (θ_2) for I=0.05, 0.10, 0.20 and 0.30A (f_d=7.4331, 7.7725, 8.97 and 10.6178 Hz), respectively and μ_A=1/4 was set.

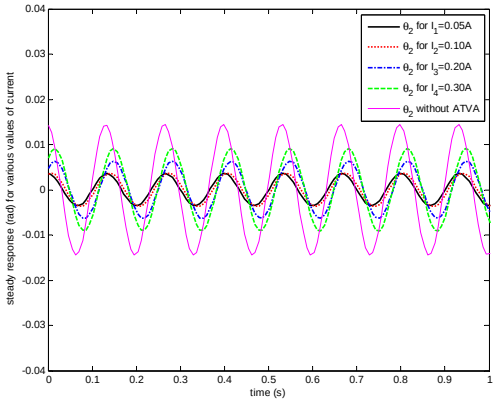

Figure 12. Steady responses of the second inertia θ_2 for several values of current I for μ_A=1/4.

It can be seen that for I=0.05A and I=0.1A, the vibrations are small ones compared to the others due to the current was tuned accurately (the exactly current I=0.072A) while for I=0.2A and 0.3A the vibrations are large. It means the input current is sensitive to the ATVA effectiveness.

Figure 13 shows the effect of damping ratio to the effectiveness of ATVA and μ_A=1/4 was set.

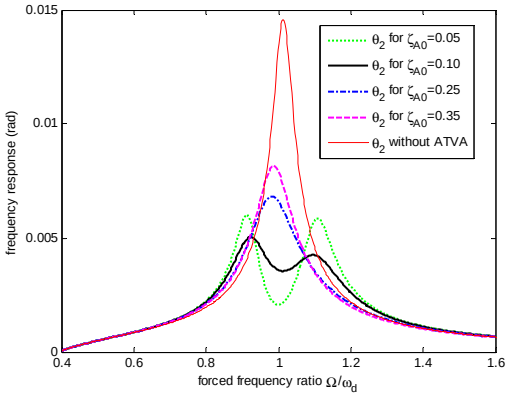

Figure 13. Responses of the second inertia for four damping ratios ς_{A0}=0.05, 0.10, 0.25 and 0.35.

Obviously, the less damping ratio is, the lower response at the resonant frequency can be. It is in agreement with the study reported by Sun et al, [24]. These authors used the theoretical approach to study a dynamic absorber and showed that the lower damping ratio is the better absorber effectiveness can be. However, a low damping ratio may results in a high vibration response at the two new invariant frequencies. For instant, for ς_{A0}=0.05 the frequency response is the smallest at ratio Ω/ω_d=1. However, at two invariant peaks the responses are higher than those when ς_{A0}=0.1. Thus, there is a demand for optimisation of the damping ratio when the ATVA work over a frequency range.

4.2 The influence of ATVA location on its effectiveness

In this section, the ATVA will be used when resonances happen to the third frequency of the second gear (f_3=28.7146Hz) and the fourth frequency of the fourth gear (f_4=68.4972Hz) as shown and noted in Table 1. At these frequencies the ATVA location is very important and it is the most essential difference between applications of ATVA for SDOF and MDOF systems. To show this more clearly, the ATVA effectiveness is compared when the ATVA location is either location A or B, where the ATVA is added to the third inertia (θ_3) as in figure 8 or to the second inertia (θ_2), respectively.

If ATVA is attached to the location B, the equation of motion keeps the same form as equation (3) with $\boldsymbol{\theta} = [\theta_1 \;\; \theta_2 \;\; \theta_3 \;\; \theta_4 \;\; \theta_A]^T$ and J=diag(J_1, J_2, J_3, J_4, J_A) and

$$\mathbf{K} = \begin{bmatrix} k_1 & -k_1 & 0 & 0 & 0 \\ -k_1 & k_1+k_2+k_A & -k_2 & 0 & -k_A \\ 0 & -k_2 & k_2+k_3 & -k_3 & 0 \\ 0 & 0 & -k_3 & k_3 & 0 \\ 0 & -k_A & 0 & 0 & k_A \end{bmatrix} \tag{15}$$

The damping matrix **C** has the same form as the stiffness matrix **K.**

For both flowing cases the inertia ratio μ_A =1/5 were set.

4.2.1 *A case study for the second gear of gear box.* In this case the engine speed is assumed to operate at 3420 rpm. The forcing frequency of fluctuation torque $T = T_0 \sin(\Omega t)$ is a half of frequency of engine, i.e., $\Omega = 2\pi \times 28.5$ (rad/s) such that the resonance happens with f_3=28.7146 Hz. The current I=0.75A (f_d=28.6847Hz) is tuned. Figure 14 shows the frequency responses for ς_{A0} =0.1, T_0 =30Nm. It is noted that the ratio range is [0.6 1.4] (forcing frequency range is [17.2108 40.1586](Hz)).

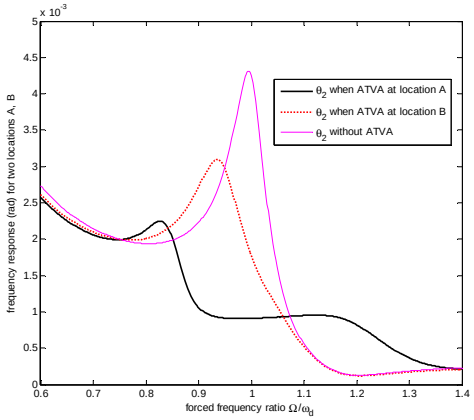

Figure 14. The responses of the second gear around a frequency range.

It can be seen that the response θ_2 when ATVA is at location A is much smaller than the others. Mean while, the response, when ATVA is located to location B, is reduced not much around the resonant frequency because the resonant frequency is not shifted away. It is confirmed that in spite of the same parameters the ATVA works effectively when it is located at location A only in this case.

4.2.2 *A case study for the fourth gear of gear box.* In this case, Ω is assumed to be 68Hz as a half of the frequency of engine speed 8160 rpm. For this speed, the fourth gear of gear box is operated. Obviously, the resonance happens to the fourth frequency f_4=68.4972Hz of the fourth gear as shown in Table 1. For this frequency the ATVA current I=2.4A (f_d=68.5337Hz) is tuned. The frequency response, when the ATVA is located to either location A or B, is shown in figure 15 for ς_{A0} =0.25, T_0 =30Nm. the ratio range is [0.6 1.4] (forcing frequency range is [41.1202 95.9472](Hz)).

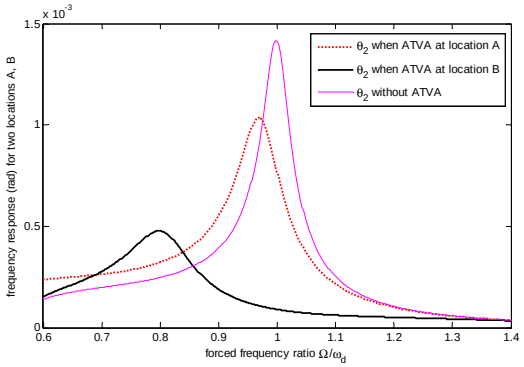

Figure 15. The powertrain frequency responses for the fourth gear around a frequency range.

In contrast to the result in section 4.2.1, the ATVA has worked effectively when it is attached to the location B only because the powertrain natural frequencies are shifted away from the resonant peaks 68.4972 Hz by introducing two new invariant frequencies. Meanwhile when ATVA is added to the location A it does not work due to the powertrain natural frequencies are not shifted and the powertrain response are reduced insignificantly at the resonant frequency.

5 Conclusion

A soft MRE is used for constructing a novel conceptual ATVA for vibration suppression of a powertrain, which is a MDOF system. Numerical results show that with the MRE material the ATVA can effectively work in a wide frequency range from around 7 to 70Hz (ten times increase in relative frequency change). In addition, this device can be properly tuned to shift powertrain natural frequencies when the gear box is set to the first, second, third and fourth gear. It is found that the MR effect in this MRE is significant so that the ATVA effectiveness is very sensitive to the input current, which is used to control the magnetic field intensity. In addition, the ATVA effectiveness is affected by not only the shear modulus (stiffness coefficient) but also by the inertia and damping ratios. When ATVA works effectively, natural frequencies of powertrain are shifted away from the forcing frequency so that powertrain steady vibration is reduced significantly. The results also show that the presented application is different from that of a SDOF, although the damping and stiffness of ATVA may be correctly tuned, the ATVA could not work well if it is not attached in a suitable location of the powertrain. The ATVA parameter optimisation and ATVA effectiveness for powertrain transient vibration reduction, when the forcing frequency varies with the time, will be our further work.

Reference

[1] Kallio M 2005 *The elastic and damping properties of magneto rheological elastomers* (VTT publications 565 Finland)

[2] Carlson J D and Jolly M R 2000 MR fluid, foam and elastomer devices *Mechatronics* 10 555–69

[3] Zhou G Y 2003 Shear properties of a magneto rheological elastomer *J. Smart Mate Struct* 12 139-46

[4] Farshad M, Benine A 2004 Magnetoactive elastomer composites *Polymer Testing* 23 347–53

[5] Zhang X, Li W and Gong X L 2008 An effective permeability model to predict field-dependent modulus of magnetorheological elastomers *J. Commu Nonlinear Sci Numer Simul* 13 1910-16

[6] Stepanov G V, Abramchuk S S, Grishin D A, Nikitin L V, Kramarenko E Y and Khokhlov A R 2007 Effect of a homogeneous magnetic field on the viscoelastic behaviour of magnetic elastomers, *Polymer* 48 488-95

[7] Abramchuk S S, Grishin D A, Kramarenko E Y, Stepanov G V and Khokhlov A R 2006 Effect of a homogeneous magnetic field on the mechanical behavior of soft magnetic elastomers under compression J. Polym. Sci., Part A 48 138-145

[8] Deng H X, Gong X, Wang L H 2006 Development of an adaptive tuned vibration absorber with magnetorheological elastomer *J. Smart Mate Struct* 15 111-16

[9] Albanese A M and Cunefare K A 2003 Properties of a magnetorheological semiactive vibration absorber *SPIE Symp.* on Smart Structures and Materials (San Diego CA) Vol 5052 36–43

[10] Lerner A A and Cunefare K A 2008 Performance of MRE-based Vibration Absorbers J. Intelligent Material Systems and Structures 19 551-563

[11] Ram Y M and Elhay S 1996 The theory of the multi-degree-of-freedom dynamic absorber *J. Sound Vibr.* 195 607-15

[12] Hadi M N S and Arfiadi Y 1998 Optimum design of absorber for MDOF structures *J. Structural Engineering* 124 1272-1280

[13] Ozer M B and Royston T J 2005 Extending Den Hartog's vibration absorber technique to multi-degree-of-freedom systems *J. Vibration and Acoustics* 127 341-50

[14] Ozer M B and Royston T J 2005 Application of Sherman–Morrison matrix inversion formula to damped vibration absorbers attached to multi-degree of freedom systems *J. Sound Vibr.* 283 1235-49

[15] Kitis L, Wang B P and Pilkey W D 1983 Vibration reduction over a frequency range *J. Sound Vibr.* 89 559-69

[16] Hwang S J, Chen J S, Liu L and Ling C C 2000 Modelling and simulation of a powertrain-vehicle system with automatic transmission *International Journal of Vehicle Design* 23 145-60

[17] Zhang N, Crowther A, Liu D K and Jeyakumaran J 2003 A finite element method for the dynamic analysis of automatic transmission gear shifting with a four-degree-of-freedom planetary gearset element *Proc. of the Instn of Mech Engrs* Part D: Journal of Automobile Engineering 217 461-73

[18] Crowther A 2004 Transient vibration in powertrain systems with automatic transmissions *Doctorate thesis University of Technolog, Sydney* Australia

[19] Couderc P, Callenaere J, Der Hagopian J, Ferraris G, Kassai A, Borjesson Y, Verdillon L and Gaimard S 1998 Vehicle driveline dynamic behaviour experimentation and simulation *J. Sound Vibr.* 218 133-57

[20] Park E J, Stoikov D, Falcao L and Suleman A 2006 A performance evaluation of an automotive magnetorheological brake design with a sliding mode controller *Mechatronics* 16 405–16

[21] Garcı´a Ta´rrago M J, Kari L, Vin˜olas J and Gil-Negrete N 2007 Torsion stiffness of a rubber bushing: a simple engineering design formula including the amplitude dependence *J. Strain Analysis for Eng design* Vol 42 13-21

[22] Wang M Y, Manoj R and Zhao W 2001 Gear rattle modelling and analysis for automotive manual transmissions Proc. of the Instn of Mech Engrs Part D: Journal of Automobile Engineering, 215 241-58

[23] Chen L, Gong X, Li X 2008 Damping of Magnetorheological Elastomers *Chin. J. Chem. Phys.* 21 581-585

[24] Sun H L, Zhang PQ, Gong X L, Chen H B 2007 A novel kind of active resonator absorber and the simulation on its control effort J. Sound Vibr. 300 117–125